Swansea University
Prifysgol Abertawe

Cronfa
Setting Research Free

Cronfa - Swansea University Open Access Repository

This is an author produced version of a paper published in :
Electrochimica Acta

Cronfa URL for this paper:
http://cronfa.swan.ac.uk/Record/cronfa29266

Paper:
Fajardo, S., Glover, C., Williams, G. & Frankel, G. (2016). The Source of Anodic Hydrogen Evolution on Ultra High Purity Magnesium. *Electrochimica Acta, 212*, 510-521.

http://dx.doi.org/10.1016/j.electacta.2016.07.018

This article is brought to you by Swansea University. Any person downloading material is agreeing to abide by the terms of the repository licence. Authors are personally responsible for adhering to publisher restrictions or conditions. When uploading content they are required to comply with their publisher agreement and the SHERPA RoMEO database to judge whether or not it is copyright safe to add this version of the paper to this repository.
http://www.swansea.ac.uk/iss/researchsupport/cronfa-support/

The Source of Anodic Hydrogen Evolution on Ultra High Purity Magnesium

S. Fajardo[a,*,1], C.F. Glover[b], G. Williams[b] and G.S. Frankel[a]

[a] Fontana Corrosion Center, Department of Materials Science and Engineering, The Ohio State University, Columbus, Ohio 43210, USA

[b] Materials Research Centre, College of Engineering, Swansea University, Bay Campus, Crymlyn Burrows, Swansea SA1 8EN, United Kingdom

Abstract

The enhanced catalytic activity of hydrogen evolution reaction on anodically polarized Mg surfaces, commonly referred to as the Negative Difference Effect, has been the topic of intense investigation in recent years. However, the cause of anodic H_2 remains unclear. To determine the primary source of H_2 evolution on dissolving Mg polarized at anodic potentials, an in-situ scanning vibrating electrode technique (SVET) analysis during galvanostatic polarization, coupled with gravimetric H_2 volume collection and potentiodynamic polarization experiments, were carried out on ultra-high purity Mg (99.9999% Mg). The combination of these methods provided solid evidence that the evolution of hydrogen on dissolving ultra-pure Mg is primarily associated with the regions dominated by the anodic reaction. Although local cathodes corresponding with the dark corrosion film formed during anodic dissolution were revealed by in-situ SVET, they appeared to play a minor role in the process.

Key Words: hydrogen evolution; magnesium; scanning vibrating electrode technique; anodic dissolution; NDE.

*Corresponding Author: fajardopanizo.1@osu.edu, santiago.fajardo@gmail.com (S. Fajardo).

[1] ISE member.

1. Introduction

The hydrogen evolution reaction (HER) occurs spontaneously on the surface of magnesium and its alloys under open circuit conditions in the presence of an aqueous electrolyte. The low open circuit potentials (OCP) exhibited by these materials, which are well below the reversible potential for HER ($E_{rev,H}$), create a large cathodic overpotential for HER and the reduction of H^+ ions (in acidic solution) or water (in neutral and alkaline solutions) is the primary cathodic reaction [1]. However, in contradiction to standard electrochemical kinetics for activation-controlled reactions, the dissolution of Mg and its alloys during anodic polarization is accompanied by persistent hydrogen evolution (HE) on the surface that increases with the amount of anodic polarization [1-3]. This high rate of HE on dissolving Mg has been termed the Negative Difference Effect but is referred to here as anodic HE. Despite intense investigations of this phenomenon [2, 4-21], the cause of this anodic HE remains unclear. Current interpretations to explain the enhancement in cathodic activation during dissolution and the source of anodic HE include three possible mechanisms based on the effect of corrosion film formation, the enrichment of impurities more noble than Mg and the effect of local anodic sites.

When pure Mg (with Fe impurity concentration below about 170 ppm) is polarized anodically from its OCP, a filiform-like attack is exhibited and a dark corrosion product forms on the electrode surface [4, 6, 22]. This corrosion film has been shown to consist of a crystalline bi-layered structure formed by an inner MgO film covered by an outer layer of $MgO/Mg(OH)_2$ [15]. Williams et al. [17] investigated anodic HE on pure Mg using the scanning vibrating electrode technique (SVET) and reported that the intense local anodic regions exhibited upon anodic polarization propagated along the electrode surface and left behind local net cathodes. Furthermore,

these local cathodes corresponded on the electrode surface with the locations of the deposited dark corrosion product formed during polarization. Salleh et al. [13] performed scanning electrochemical microscopy (SECM) and cathodic polarization measurements on a $Mg(OH)_2$ coated Mg electrode and found larger HE rates than those on the uncoated surface. These findings provide experimental evidence for the concept that, during Mg anodic polarization, the HER is enhanced on the dark corrosion film, which is therefore the location of the anodic HE.

The effect of noble metal impurities on Mg corrosion and HE has been known for a long time [23], but the notion that they may be the source of anodic HE has been the subject of recent investigations. It is hypothesized that impurities more noble than Mg accumulate on its surface during dissolution and act as preferential cathodic sites for the HER. Based on findings of very small iron particles on the surface of corroded high purity Mg [15], Lysne et al. [10] proposed a model for the Fe enrichment efficiency on Mg specimens with different concentrations of Fe after anodic dissolution. They found Fe enrichment efficiency to be very poor and unable to explain the large amount of H_2 produced at potentials above the OCP. These findings were supported by Cain et al. [7] who studied Fe enrichment efficiency on previously corroded pure Mg specimens by Rutherford Backscattering Spectrometry (RBS). Despite detecting Fe enrichment of about one order of magnitude, the total concentration of Fe remained far below 1 at.%. Höche et al. [19] proposed a mechanism where Fe impurities in a pure Mg specimen (even at concentrations below 100 ppm) may leave the surface due to preferential dissolution of Mg and redeposit on the electrode surface after self-corrosion at their OCP. This mechanism, similar to that occurring on AA2024 with Cu-rich intermetallic particles [24], would create re-deposited Fe films that could drive the cathodic current and become the primary source of anodic H_2. However, increased areas of such Fe-rich

patches on the dissolving Mg surface are not consistent with the observation of a HE rate that is constant with time for a given fixed anodic current density. It is also not clear if noble metal re-deposition can account for the remarkably high rates of HE exhibited by ultra-high purity dissolving Mg (~0.1 ppm Fe) [4]. Furthermore, Fe deposition could be considerably affected by the intense convection in the electrolyte due to the copious evolution of H_2 during anodic dissolution, particularly at large polarizations. Anodic HE was recently measured on electrodes of both high purity (99.98% Mg) and ultra-high purity Mg (99.9999% Mg) [4]. Even the ultra-high purity Mg material with a total impurity content of ~1 ppm exhibited extremely high HE rates, confirming that this phenomenon cannot be fully explained in terms of impurity enrichment.

Finally, the role of dissolving anodic sites on HE at anodic potentials has also been investigated. Frankel et al. [8] proposed that the enhanced rates of HE may be a result of an increase in the exchange current density for the HER on Mg ($i_{0,H,Mg}$) as the rate of Mg dissolution increases. In this model, $i_{0,H,Mg}$ is considered a dynamic parameter instead of constant. This notion has also been applied to explain anodic HE in Al pits and on dissolving Al in concentrated acid solutions [2]. Although the underlying mechanism for this behavior is not yet clear, changes in the surface nature of dissolving Mg regions may influence its chemical reactivity, increasing the HER kinetics. This hypothesis has been supported in a recent study [4] where the contribution of the dark corrosion product on Mg and/or the enrichment of noble elements to the total amount of hydrogen collected during anodic polarization was estimated. For that purpose, it was assumed that the corrosion film and the accumulated impurities formed during dissolution are robust in that they are relatively unchanged during subsequent cathodic polarization. Extrapolation of the behavior in the cathodic region to the potentials

reached during anodic polarization proved that the HE rate associated with the accumulated products (i.e. corrosion product and impurities enriched at the surface) was small during anodic polarization. The enhanced catalytic activity for the HER on dissolving Mg was found to be primarily associated with the regions dominated by the anodic dissolution reaction.

The aim of the present paper is to make advancements in elucidating the source of anodic HE and contribute to the general understanding of persistent evolution of hydrogen on anodically polarized Mg. For that purpose, the effects of anodic dissolution on ultra-high purity Mg specimens were investigated by SVET, H_2 collection and electrochemical measurements. The influence of anodic regions and corrosion film on the catalytic activity for the HER is discussed.

2. Experimental

Ultra-high purity (UHP) Mg was used as test specimen. UHP Mg was obtained from United Mineral and Chemical Corporation (NJ, USA). This material, with a nominal purity of 99.9999%, was used in a previous work and its chemical composition is given elsewhere [4]. It is worth noting that the concentration of Fe was 0.1 ppm. Samples with a Cu wire attached to the back were cold mounted in epoxy resin and ground under ethanol to 1200 grit using silicon carbide papers. The samples used for SVET measurements were then masked with 90 μm thick extruded PTFE 5490 tape (3 M Ltd), such that only about 5×5 mm square area was exposed to electrolyte. A 2 M NaCl solution at pH~6 was used as electrolyte. All solutions were prepared from laboratory grade reagents and with high purity water of 18.2 MΩ cm (Millipore™ system).

SVET measurements were carried out using a probe comprising a 125 μm diameter platinum wire sealed in a glass sheath so that the active portion of the probe tip consisted of a 125 μm diameter Pt micro-disc electrode. The probe vibration frequency was 140 Hz and the peak-to-peak vibration amplitude was 30 μm. Full details of the SVET instrument design, mode of operation and calibration procedure to give values of current flux density along the axis of probe vibration (j_z) are given elsewhere [25]. A total net charge of 6 C cm^{-2} was passed galvanostatically at different anodic current densities in the range of 1 to 4 mA cm^{-2} by means of an in-house micro-galvanostat. SVET scans were performed at a constant height by holding the probe vertically 100 μm above the metal surface. Numerical area integration of j_z distributions per scan was carried out to calculate the time-dependent total measured cathodic current (I_c), according to a protocol described in detail elsewhere [17, 25]. After normalization by the nominal surface area of the electrode, this allows the evolution of the time-dependent area-averaged cathodic current density (i_c) during the time of galvanostatic current density application to be determined.

Hydrogen collection measurements were conducted using the gravimetric method originally developed by Curioni [26] and described previously [27]. The gravimetric method is based on the buoyant force exerted by the H_2 produced by dissolving Mg when the gas is accumulated in a submerged container. The gravimetric method exhibits higher sensitivity in HE detection than the volumetric method and allows for hydrogen volume collection during polarization measurements with high temporal resolution. Anodic HE was investigated during galvanostatic polarization measurements by the application of the same anodic current densities used in the SVET experiments (i.e. from 1 to 4 mA cm^{-2}).

To study the effect of the amount of corrosion product on the catalytic activity of the UHP Mg surface after anodic treatment, galvanostatic polarization experiments were carried out in 0.1 M NaCl solution passing different charges at a constant applied anodic current density of 10 mA cm^{-2}.

The OCP of the samples was monitored for 15 minutes prior to the application of the polarization signals to allow the system to reach both a stable potential and, in the case of the gravimetric experiments, also a steady weight.

Cathodic potentiodynamic polarization curves were measured immediately after the anodic galvanostatic treatments. For these experiments the electrolyte was replaced by fresh solution (i.e. 0.1 M or 2 M NaCl) and the cathodic polarization measurement was performed scanning downwards to 700 mV below the OCP at 1 mV/s.

All electrochemical tests were performed using a conventional three-electrode configuration with the UHP Mg sample acting as the working electrode, a Pt mesh as the counter electrode and a saturated calomel electrode (SCE) as the reference electrode. A Gamry Instruments Reference 600 potentiostat/galvanostat controlled by the Gamry Framework software was used to perform the electrochemical experiments.

All experiments were repeated at least two times and were found to be reproducible.

3. Results

3.1. Scanning Vibrating Electrode Technique (SVET) measurements

Figs. 1-3 show typical SVET-derived surface maps of local current density along the axis of probe vibration (j_z) above a UHP Mg surface during the galvanostatic application of anodic current densities of 1, 2, and 4 mA cm^{-2}, respectively, in 2 M NaCl solution as a function of time. A total net charge of 6 C cm^{-2} was passed in each

case. The images in Figs. 1-3 represent the evolution of the electrochemical activity of the surfaces and were not taken at times of equal charge passed. Intense local anodic sites were observed on the electrode surfaces during the initial scan at the early stages of polarization. Localized attack resulted from the chloride-induced breakdown of the native oxide film present on the UHP Mg surface.

As previously observed on high purity Mg immersed in 2 M NaCl solution [17], the progression of the local anodic regions across the UHP Mg electrode surface left behind regions dominated by net cathodic activity. With time of polarization, the fraction of the surface above which net cathodic current densities where detected by SVET increased. The SVET data in Figs. 1-3 were numerically integrated using the approach described previously [17, 25] to determine the time-dependent total measured cathodic current density for each scan as shown in Fig. 4. An increase in the integrated cathodic current density was observed in all cases with polarization time after the local cathodes appeared on the UHP Mg surface. The time needed for these local cathodes to become established exhibited a clear dependence on the magnitude of the applied anodic current. For the highest applied current densities, local cathodic activity was exhibited from the early stages of polarization (detected on first scan) whereas for the lowest applied current density (i.e. +1 mA cm^{-2}) there was a delay of about 20 min. The intensity of the integrated total cathodic current density from SVET also increased with larger applied anodic current density at a given time. The sharp increase in the integrated cathodic current for the 4 mA cm^{-2} sample is likely caused by a spatial resolution issue. Figs. 3a-c show two rings of anodic current that increased in diameter with time. When these rings were small, it is likely that the SVET could not resolve the cathodic current left behind so that the real cathodic current was larger than the measured value at short times.

Fig. 5 shows the surface appearance of the UHP Mg electrode after the SVET measurements at different anodic current densities to a net charge of 6 C cm^{-2}. The filiform-like dark corrosion product typically exhibited during dissolution of high purity Mg was observed. As previously reported by Williams et al. [17], a correspondence between the regions covered with the dark corrosion product and the sites on the surface where net cathodic activity was detected by SVET can be observed. This confirms the enhanced electro-catalytic properties of the corrosion film formed during Mg dissolution with respect to the native Mg surface towards the HER.

Considering that the dark regions are sites of net cathodic current, these observations along with other independent studies have been adopted as evidence of the role of the dark corrosion film as the source of the enhanced anodic HE rates exhibited by dissolving Mg specimens [13, 17, 26]. The role of the film in the occurrence of anodic H_2 will be discussed below.

3.2. Gravimetric hydrogen volume collection experiments under galvanostatic polarization

Fig. 6 shows the volume of hydrogen collected during the application of different current densities as a function of time for the UHP Mg in 2 M NaCl as calculated from the gravimetric data. Data from duplicated experiments are presented. The evolution of hydrogen volume was linear in all cases. However, an initiation period of lower volume was exhibited at the early stages of polarization for the lowest applied current densities. Hydrogen is very soluble in aqueous solutions [9, 28]. As a result, despite the high sensitivity of the gravimetric method, it is likely that the hydrogen evolved in the first stages of experimentation was in part dissolved in the electrolyte, resulting in lower HE rates detected in the first minutes. After the initial period, the HE

rate on each electrode surface reached a constant value, which has been observed previously [4, 8, 14, 17, 27]. Note that this constant rate of anodic HE is in contradiction with the increasing rate of HE measured by integration of the SVET data, and suggests that the SVET measurements are not directly related to the anodic HE.

The linear portions of the HE curves were used to determine the steady state HE current densities using Faraday's Law. Fig. 7 shows the calculated current densities associated with HE as a function of the applied current density for the UHP Mg electrode in 2 M NaCl solution. Hydrogen evolution current density increased linearly with increasing applied anodic current density, representing approximately a 44% of the latter. This is in agreement with observations reported in a previous work using the same Mg purity in 0.1 M NaCl [4]. It is worth noting that, although the initiation period was slightly different between duplicated experiments for a given current density applied, highly reproducible steady state values were observed.

Fig. 8 shows the macroscopic appearance of the UHP Mg electrode after a charge of 6 C cm^{-2} was passed at different anodic current densities in 2 M NaCl solution using the gravimetric method. Typical filiform tracks of dark corrosion product were exhibited in all cases. The dark corrosion product covered approximately half of the electrode surface for the lowest applied current density. As reported in a previous work, the surface coverage slightly increased with increasing the applied current density even for a constant net charge passed [4]. It is interesting to note that, although the electrode surface became increasingly covered with corrosion product during the time of current application, the current density values associated with HE remained constant. This observation is also not consistent with the notion that the corrosion film is entirely responsible for the occurrence of anodic H_2. In such a case, a nonlinear-like evolution of

the hydrogen volume should be expected as surface coverage increases with time of polarization.

3.3. Cathodic polarization experiments on previously-polarized Mg surfaces

With the aim of evaluating the HE kinetics on the previously corroded UHP Mg surfaces, cathodic potentiodynamic polarization measurements were carried out immediately after the anodic polarization was finished. This approach, also developed in a previous work [4], was originally proposed by Birbilis and Taheri et al. [6, 15] in parallel investigations where the catalytic activity for HER on a pure Mg surface was studied prior and following anodic dissolution in 0.1 M NaCl.

Fig. 9 shows the cathodic potentiodynamic polarization curves for the UHP Mg electrode in 2 M NaCl solution after galvanostatic polarization at different anodic current densities to a charge of 6 C cm^{-2}. The curves were highly reproducible so only one curve is presented for each condition. The response of the UHP Mg with no prior anodic polarization is also presented for comparative purposes. Cathodic polarization curves were measured immediately after the anodic galvanostatic experiments were finished. As described in a previous work [4], replacement of the electrolyte was carried out before the start of the potentiodynamic experiments to prevent any influence on the local pH that prior anodic polarization may have induced. In contrast with previous observations using the UHP Mg material in 0.1 M NaCl [4] where a slight enhancement in the cathodic current density was exhibited for previously-polarized samples, no significant differences were observed for the curves after anodic polarization at different anodic current densities when 2 M NaCl solution was used. This indicates comparable catalytic activity of their surfaces for the HER. When the response of the previously polarized samples is compared to that with no prior polarization, a shift in the E_{corr}

towards more positive potential values was observed. The higher E_{corr} exhibited by the corroded surfaces with respect to the non-polarized one was likely due to a decrease in the anodic kinetics, resulting in a net cathodic current measured in the region that was previously dominated by the anodic Mg dissolution reaction. This is interesting because it suggests that the dark corrosion product formed during anodic polarization was able to partially protect the UHP Mg surface. Another interesting feature is that in 0.1 M NaCl a clear enhancement in the cathodic kinetics was exhibited for previously-polarized samples compared to a fresh surface [4], whereas this was not the case in 2 M NaCl.

It is possible to determine the HE current density associated with the corrosion film during anodic polarization. For this purpose, extrapolation of the Tafel line in the cathodic region to the potentials reached during anodic polarization was carried out, as presented previously [4]. This protocol is based in the assumption that the corrosion film formed during Mg dissolution and the accumulated impurities do not change significantly during subsequent cathodic polarization. It is worth noting that accumulation of noble impurities is unlikely to play a role given the extremely high purity of the UHP Mg material (~1 ppm total impurity concentration), which represents the behavior of pure Mg as much is possible. Fig. 10 shows an example of the analysis for the case of prior polarization at 1 mA cm^{-2}. The intense HE occurring at the electrode surface causes large ohmic potential drops and distorts the shape of the polarization curve, making determination of accurate Tafel regions to carry out the extrapolation quite difficult. For this reason, two different Tafel lines, referred to for clarity as upper and lower limit approximation, were considered. Note that this analysis was performed not too far from the OCP as ohmic potential drop increases with increasing cathodic polarization. The real contribution of the dark corrosion film to the

HE current density will be between the limits of these two. In Fig. 10 the lines are extrapolated to -1.694 V_{SCE}, which is the steady-state, IR-corrected, potential that was measured during prior anodic polarization at 1 mA cm^{-2}. Different steady-state potentials were measured during anodic polarization at 2 and 4 mA cm^{-2}. The cathodic Tafel lines for these samples were extrapolated to the respective steady state potentials. The IR correction associated with the abundant HE was performed during the galvanostatic experiment by the current interrupt method.

Fig. 11 shows the HE current density values associated with the corrosion product for the UHP Mg electrode in 2 M NaCl under the application of different anodic current densities. Very similar values with a difference of only about 30-40 µA cm^{-2} were observed for the upper and lower limit approximations. A slight increase of the HE current density with the applied anodic current density was observed. However, it is worth noting that this increase (~20 µA cm^{-2} between the lowest and highest applied current densities) was remarkably smaller than the influence of applied anodic current on the hydrogen gas evolution (see Fig. 7).

4. Discussion

To successfully explain the enhanced catalytic activity for the HER on dissolving Mg, it is necessary to determine the primary source of H_2 gas. The total current density associated with the HER can be described by the summation of the individual contributions to the HE current density of all the local sites that may support the evolution of anodic H_2 [4]:

$$i_{TOT} = i_{Anod} + i_{Film} + i_{\mathrm{Im}\,p} \quad (1)$$

where i_{TOT} is the total HE current density obtained using the gravimetric method for H_2 volume collection (see Fig. 7) and i_{Anod}, i_{Film} and i_{Imp} are the individual contributions to

the total HE current density associated with the regions dominated by the net anodic reaction, the dark corrosion film and the accumulation of noble impurities on the electrode surface, respectively. It is necessary to note that i_{Anod} cannot be determined directly. However, it can be calculated by the difference between i_{TOT} and the summation of i_{Film} and i_{Imp}, according to Eq. (1). It is not possible to discern between i_{Film} and i_{Imp} by the experimental approaches used in the present investigation so they will be considered as a single contribution and referred to as $i_{Film+Imp}$ for simplicity. However, considering the extremely low concentration of impurities present in the UHP Mg material (~1 ppm), it is reasonable to consider that the contribution of i_{Imp} is very small.

Figs. 12-14 show a compilation of all the cathodic current density values calculated in the previous section by different methods for the UHP Mg under galvanostatic polarization at different applied anodic current densities in 2 M NaCl solution plotted as a function of time. The blue curves that show noise in each figure are the instantaneous measurements of the total HE current density values, $i_{TOT,Ins.}$, determined by the gravimetric method during galvanostatic polarization experiments. In contrast with the smoothed curves shown in Fig. 6, a noisy signal was observed for the instantaneous HE current density (see Figs. 12-14). The reason for this is that while Fig. 6 shows cumulative data, the instantaneous HE current density was calculated from the slope of consecutive individual measurements recorded in a small time scale.

The red lines in Figs. 12-14 show the total cathodic current densities calculated by numerical integration of the SVET maps (i_{SVET}). The green bands represent the range of contribution to the HE expected from the dark film and impurities, as determined by extrapolation of the cathodic curves to the respective IR-corrected anodic potentials. Figures 12-14 therefore represent the HE data from three separate techniques:

gravimetric HE data, integrated SVET data, and extrapolated cathodic polarization curves. Representation of the all cathodic currents occurring at the electrode surface during Mg dissolution provide valuable information about the primary source of HE as it allows for direct comparison of the individual contributions to the total HE current density.

For each i_{app}, the predicted HE for the dark film and impurities calculated by extrapolation of the cathodic polarization curve, $i_{Film+Imp}$, exhibited a very good agreement with the i_{SVET} values detected at the end of anodic polarization. Note that the cathodic polarization curves were measured immediately after the anodic polarization finished and so they represent the behavior of the electrode surface in a situation comparable with that detected by SVET at the final stages of the galvanostatic experiment. The correspondence of the extrapolated polarization curves and integrated SVET data suggests that both approaches accurately measure the HER associated with the dark product and impurities.

However, Figs. 12-14 also show that the total rate of HE as determined gravimetrically was significantly higher than $i_{Film+Imp}$ for all the applied anodic current densities, with differences of one order of magnitude observed for the highest values of i_{app} (i.e. +2 and +4 mA cm^{-2}). Note that $i_{Film+Imp}$ decreased from 20% to 7% of the total HE current density as i_{app} increased from +1 and +4 mA cm^{-2}, indicating that for the highest current density applied, over 90% of i_{TOT} was not from $i_{Film+Imp}$. This provides solid evidence that, even though the dark corrosion film exhibits enhanced catalytic activity for the HER, its contribution to the total anodic HE current density is small and further supports the notion that the dark corrosion product is not responsible for causing the enhanced rates of anodic HE on anodically polarized Mg. $i_{TOT,Inst.}$ exhibited lower values within the first minutes of polarization for the same reason that the H_2 collected

shown in Fig. 6 exhibited an initiation period of lower volume at the early stages of the measurement as described above.

Fig. 15 shows the total HE current density from gravimetric measurements, along with the components associated with the dissolving anodic sites and with the film/impurities as a function of applied anodic current density. i_{Anod} values were slightly lower than i_{TOT}, whereas $i_{Film+Imp}$ was much smaller and relatively independent of the applied current density. This is reasonable considering that the same charge was passed and the surface appearances of the electrodes after the galvanostatic polarization experiments at different anodic current densities were relatively comparable (see Fig. 8). These results are in agreement with a previous study where a similar behavior was observed for the UHP Mg in 0.1 M NaCl solution [4] and confirm that the primary source for anodic HE are the regions dominated by the Mg dissolution reaction. Furthermore, because the majority of HE occurs at or near the regions where Mg is actively dissolving, anode to cathode spacing will be significantly less than the SVET probe scan height of 100 μm. In such a scenario, any ionic current loops coupling anodic Mg dissolution with cathodic HE will pass well below the plane of scan and as such remain undetected by SVET [29]. Furthermore, the SVET detects electrochemical activity, so that any local cathodic current occurring at a region dominated by net anodic dissolution will also remain unrevealed. This therefore explains why i_{SVET} represents only a fraction of the instantaneous current density associated with HE ($i_{TOT,\ Inst}$), and demonstrates that for the highly pure form of Mg studied here, long range (> 100 μm) coupling between local anode sites and cathodic HE on the dark film plays a relatively small role. It is worth noting that, despite the linear response exhibited by the curves in Fig. 6 after the initial period of polarization (straight lines with correlation coefficients ≥0.997 for all cases), a continuous increase of $i_{TOT,Inst.}$ was observed in Figs. 12-14

(particularly Figs. 12 and 13) within the period of time where linearity was shown. However, this increase is small relative to the high rates of HE on the surface.

With the aim of further investigating the role of the dark corrosion film on the enhanced catalytic activity for the HER of dissolving Mg surfaces, complementary galvanostatic experiments were performed on anodically polarized UHP Mg surfaces in which different charges in the range of 1 to 30 C were passed at a single anodic current density, 10 mA cm^{-2}. According to Faraday's law, the amount of metal dissolved will be directly proportional to the charge passed through the electrode. Mg does not strictly follow Faraday's law as a consequence of the anodic HE. However, rate of anodic HE is relatively constant with time or charge. Consequently, greater charges passed will result in more metal dissolved and, as will be shown below, in more corrosion product deposited on the corroding surface. If the dark corrosion film were to be the driving element for anodic HE, increased rates of HE should be exhibited for longer current application times. Furthermore, enhanced cathodic kinetics would be expected when polarizing the samples cathodically after the galvanostatic treatment as charge passed increases. Cain et al. [7] and Curioni et al. [30] performed similar tests on Mg of commercial purity and found enhanced cathodic activity after anodic potentiostatic polarization. However, it is of interest to investigate the role of the corroded surface on the UHP Mg used in this study, as any possible effect coming from the accumulation of noble impurities can be reasonably discarded and the effect of the film alone can be accurately investigated.

Fig. 16 shows the volume of hydrogen collected during galvanostatic polarization for the UHP Mg in 0.1 M NaCl using the gravimetric method for H_2 volume collection plotted as a function of time. Data from duplicate experiments are presented, showing that the results were highly reproducible. As previously observed,

the volume of H_2 increased linearly with time in all cases with no period of lower HE rates. However, for the greatest charge passed (i.e. 30 C), a slight increase in the volume of H_2 collected after about 20 min was observed. It is likely that this was the time for the electrolyte to become fully saturated with H_2. Furthermore, as described in a previous study, it is also possible that after that period of time the bubbling of the electrolyte with the produced H_2 gas may lead to removal of other gases dissolved in it (i.e. O_2 and N_2) [27]. In any case, as observed in Fig. 17, the HE current density values were very similar with less than a 2X increase in the steady-state HE current density over the whole range of charge passed. However, the charge passed increased by a factor of 30.

Fig. 18 shows the surface appearance of the UHP Mg surface after different charges were passed at 10 mA cm^{-2} in 0.1 M NaCl solution. Typical filiform-like tracks formed in all cases. The electrode surface was progressively more covered with dark corrosion product as the net charge increased. A higher magnification is provided in Fig. 19 for the UHP Mg surface after 1 and 30 C. The surface appearance changed remarkably with the time of polarization at +10 mA cm^{-2}. After 1 C was passed, small and relatively uniform localized corrosion features were exhibited on the electrode surface. However, a heavily corroded surface was observed on the UHP Mg when the greatest charge was passed. Furthermore, a white solid was deposited on the electrode surface after a charge of 30 C was passed. This white corrosion product was observed on replicated experiments. No analysis of this precipitate was carried out but, according to previous observations, it is likely that this product was $Mg(OH)_2$ [4]. When the white solid was removed with a cotton-tipped swab soaked in ethanol, a dense oxide film covering almost the entire electrode surface was revealed. It should be noted that in contrast with the noticeable increase in the extent of the electrode surface covered with

dark corrosion product, the HE current densities calculated by H_2 volume collection (Fig. 17) were only slightly increased.

Fig. 20 shows the cathodic potentiodynamic polarization curves for the UHP Mg electrode in 0.1 M NaCl solution after galvanostatic polarization passing different charges at a constant anodic current density of 10 mA cm^{-2}. Typical results from replicate experiments are presented. The cathodic potentiodynamic response of the UHP Mg electrode in 0.1 M NaCl in the absence of prior anodic polarization is also presented for comparative purposes. Increased cathodic kinetics was observed after the galvanostatic treatment was performed, even for the lowest net charge passed. However, almost no difference in the polarization curves was observed for samples subjected to prior anodic dissolution, presenting very similar current density values over the whole range of potentials applied below the OCP. Considering the big differences exhibited in Figs. 19 and 20 in the amount of film covering the electrode surface, these observations confirm the enhanced catalytic behavior of the corrosion film that originates during anodic polarization but, more importantly, provide evidence that the film plays a minor role in the evolution of hydrogen at anodic potentials.

5. Conclusions

SVET and galvanostatic measurements coupled with gravimetric H_2 volume collection and potentiodynamic polarization experiments were carried out on ultra-high purity Mg (99.9999% Mg) to determine the primary source of H_2 evolution on dissolving Mg polarized at anodic potentials from the OCP. The role of the dark corrosion film in the process was also investigated. The following can be concluded:

- The total cathodic current density calculated by integration of the SVET-derived surface maps along the axis of probe vibration (j_z) during anodic polarization of the

UHP Mg exhibited a very good agreement with the HE current density associated with the dark corrosion film and the accumulation of noble impurities on the electrode surface as determined by extrapolation of subsequent cathodic polarization curves to the anodic potential. This indicates that both approaches accurately measure the HER associated with the dark product and impurities.

- The total rate of HE determined using the gravimetric method was significantly higher than the HE current density associated with the dark product and impurities for all the applied anodic current densities.
- Greater net charges passed at a single anodic current density originated increased corrosion product formation on the electrode surface. However, a very small impact on the catalytic activity for the HER was exhibited.
- The evolution of hydrogen on anodically polarized Mg is primarily associated with the regions dominated by the anodic dissolution reaction. Within these regions, sites of anodic Mg dissolution coupled with cathodic hydrogen evolution are not physically separable and therefore cannot be detected by SVET.

Acknowledgements

G. Williams and C.F. Glover recognize the financial support of the EPSRC, Welsh Government and Innovate UK for the SPECIFIC Innovation and Knowledge Centre (grant numbers EP/I019278/1, EP/K000292/1, EP/L010372/1).

References

[1] S. Thomas, N.V. Medhekar, G.S. Frankel, N. Birbilis, Corrosion mechanism and hydrogen evolution on Mg, Curr. Opin. Solid State Mat. Sci. 19 (2015) 85.

[2] G.S. Frankel, S. Fajardo, B.M. Lynch, Introductory lecture on corrosion chemistry: a focus on anodic hydrogen evolution on Al and Mg, Faraday Discuss. 180 (2015) 11.

[3] A. Atrens, W. Dietzel, The negative difference effect and unipositive Mg, Adv. Eng. Mater. 9 (2007) 292.

[4] S. Fajardo, G.S. Frankel, Effect of impurities on the enhanced catalytic activity for hydrogen evolution in high purity magnesium, Electrochim. Acta 165 (2015) 255.

[5] N. Birbilis, T. Cain, J.S. Laird, X. Xia, J.R. Scully, A.E. Hughes, Nuclear Microprobe Analysis for Determination of Element Enrichment Following Magnesium Dissolution, ECS Electrochem. Lett. 4 (2015) C34.

[6] N. Birbilis, A.D. King, S. Thomas, G.S. Frankel, J.R. Scully, Evidence for enhanced catalytic activity of magnesium arising from anodic dissolution, Electrochim. Acta 132 (2014) 277.

[7] T. Cain, S.B. Madden, N. Birbilis, J.R. Scully, Evidence of the Enrichment of Transition Metal Elements on Corroding Magnesium Surfaces Using Rutherford Backscattering Spectrometry, J. Electrochem. Soc. 162 (2015) C228.

[8] G.S. Frankel, A. Samaniego, N. Birbilis, Evolution of hydrogen at dissolving magnesium surfaces, Corros. Sci. 70 (2013) 104.

[9] A.D. King, N. Birbilis, J.R. Scully, Accurate Electrochemical Measurement of Magnesium Corrosion Rates; a Combined Impedance, Mass-Loss and Hydrogen Collection Study, Electrochim. Acta 121 (2014) 394.

[10] D. Lysne, S. Thomas, M.F. Hurley, N. Birbilis, On the Fe Enrichment during Anodic Polarization of Mg and Its Impact on Hydrogen Evolution, J. Electrochem. Soc. 162 (2015) C396.

[11] L. Rossrucker, K.J.J. Mayrhofer, G.S. Frankel, N. Birbilis, Investigating the Real Time Dissolution of Mg Using Online Analysis by ICP-MS, J. Electrochem. Soc. 161 (2014) C115.

[12] L. Rossrucker, A. Samaniego, J.-P. Grote, A.M. Mingers, C.A. Laska, N. Birbilis, G.S. Frankel, K.J.J. Mayrhofer, The pH Dependence of Magnesium Dissolution and Hydrogen Evolution during Anodic Polarization, J. Electrochem. Soc. 162 (2015) C333.

[13] S.H. Salleh, S. Thomas, J.A. Yuwono, K. Venkatesan, N. Birbilis, Enhanced hydrogen evolution on Mg (OH)2 covered Mg surfaces, Electrochim. Acta 161 (2015) 144.

[14] A. Samaniego, N. Birbilis, X. Xia, G.S. Frankel, Hydrogen Evolution During Anodic Polarization of Mg Alloyed with Li, Ca, or Fe, Corrosion 71 (2014) 224.

[15] M. Taheri, J.R. Kish, N. Birbilis, M. Danaie, E.A. McNally, J.R. McDermid, Towards a Physical Description for the Origin of Enhanced Catalytic Activity of Corroding Magnesium Surfaces, Electrochim. Acta 116 (2014) 396.

[16] S. Thomas, O. Gharbi, S.H. Salleh, P. Volovitch, K. Ogle, N. Birbilis, On the effect of Fe concentration on Mg dissolution and activation studied using atomic emission spectroelectrochemistry and scanning electrochemical microscopy, Electrochim. Acta 210 (2016) 271.

[17] G. Williams, N. Birbilis, H.N. McMurray, The source of hydrogen evolved from a magnesium anode, Electrochem. Comm. 36 (2013) 1.

[18] G. Williams, N. Birbilis, H.N. McMurray, Controlling factors in localised corrosion morphologies observed for magnesium immersed in chloride containing electrolyte, Faraday Discuss. 180 (2015) 313.

[19] D. Hoche, C. Blawert, S.V. Lamaka, N. Scharnagl, C. Mendis, M.L. Zheludkevich, The effect of iron re-deposition on the corrosion of impurity-containing magnesium, Phys. Chem. Chem. Phys. 18 (2016) 1279.

[20] S. Lebouil, O. Gharbi, P. Volovitch, K. Ogle, Mg Dissolution in Phosphate and Chloride Electrolytes: Insight into the Mechanism of the Negative Difference Effect, Corrosion, 71 (2015) 234.

[21] Y. Yang, F. Scenini, M. Curioni, A study on magnesium corrosion by real-time imaging and electrochemical methods: relationship between local processes and hydrogen evolution, Electrochim. Acta 198 (2016) 174.

[22] K.D. Ralston, G. Williams, N. Birbilis, Effect of pH on the Grain Size Dependence of Magnesium Corrosion, Corrosion 68 (2012) 507.

[23] R.E. McNulty, J.D. Hanawalt, Some Corrosion Characteristics of High Purity Magnesium Alloys, ECS Trans. 81 (1942) 423.

[24] R.G. Buchheit, R.P. Grant, P.F. Hlava, B. Mckenzie, G.L. Zender, Local Dissolution Phenomena Associated with S Phase (Al2CuMg) Particles in Aluminum Alloy 2024-T3, J. Electrochem. Soc. 144 (1997) 2621.

[25] G. Williams, H. Neil McMurray, Localized Corrosion of Magnesium in Chloride-Containing Electrolyte Studied by a Scanning Vibrating Electrode Technique, J. Electrochem. Soc. 155 (2008) C340.

[26] M. Curioni, The behaviour of magnesium during free corrosion and potentiodynamic polarization investigated by real-time hydrogen measurement and optical imaging, Electrochim. Acta 120 (2014) 284.

[27] S. Fajardo, G.S. Frankel, Gravimetric Method for Hydrogen Evolution Measurements on Dissolving Magnesium, J. Electrochem. Soc. 162 (2015) C693.

[28] S. Lebouil, A. Duboin, F. Monti, P. Tabeling, P. Volovitch, K. Ogle, A novel approach to on-line measurement of gas evolution kinetics: Application to the negative difference effect of Mg in chloride solution, Electrochim. Acta 124 (2014) 176.

[29] G. Williams, A.J. Coleman, H.N. McMurray, Inhibition of Aluminium Alloy AA2024-T3 pitting corrosion by copper complexing compounds, Electrochim. Acta 55 (2010) 5947.

[30] M. Curioni, F. Scenini, T. Monetta, F. Bellucci, Correlation between electrochemical impedance measurements and corrosion rate of magnesium investigated by real-time hydrogen measurement and optical imaging, Electrochim. Acta 166 (2015) 372.

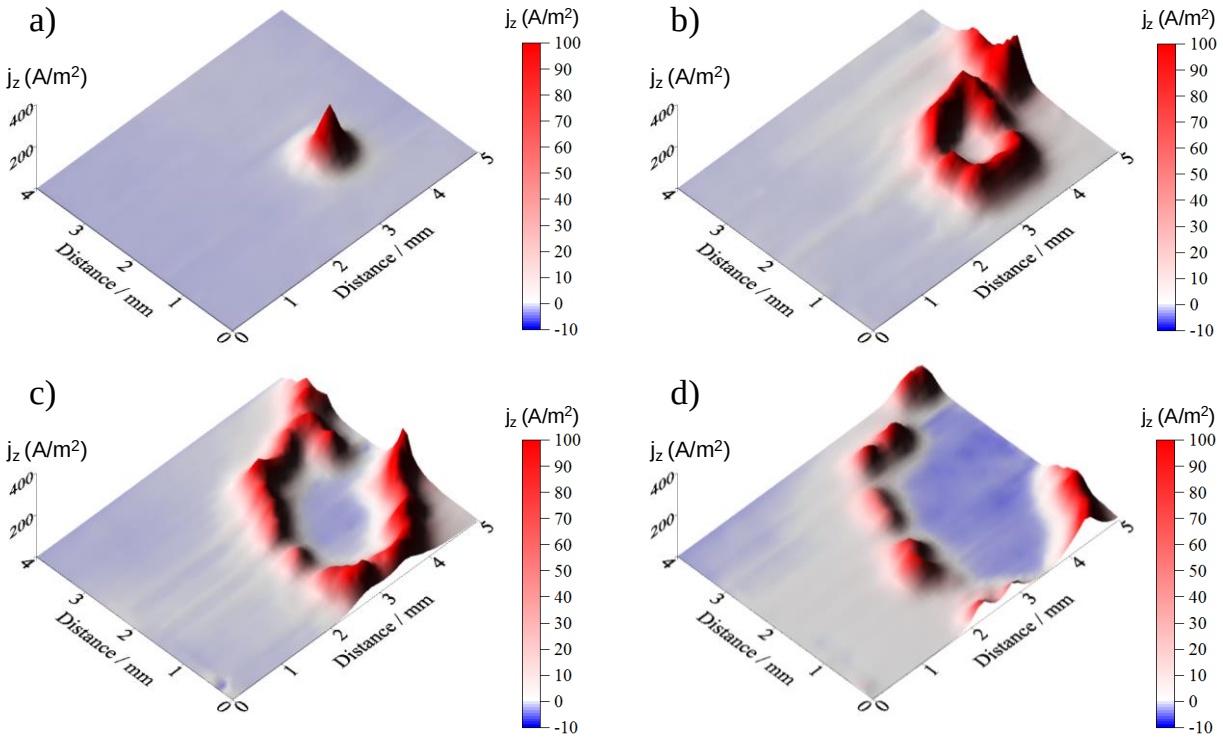

Fig. 1.Surface maps showing normal current density (j_z) distributions above a UHP Mg surface immersed in a 2 M NaCl solution, (a) 7, (b) 35, (c) 63 and (d) 98 min after starting galvanostatic polarization at +1 mA cm^{-2}. A net charge of 6 C cm^{-2} was passed.

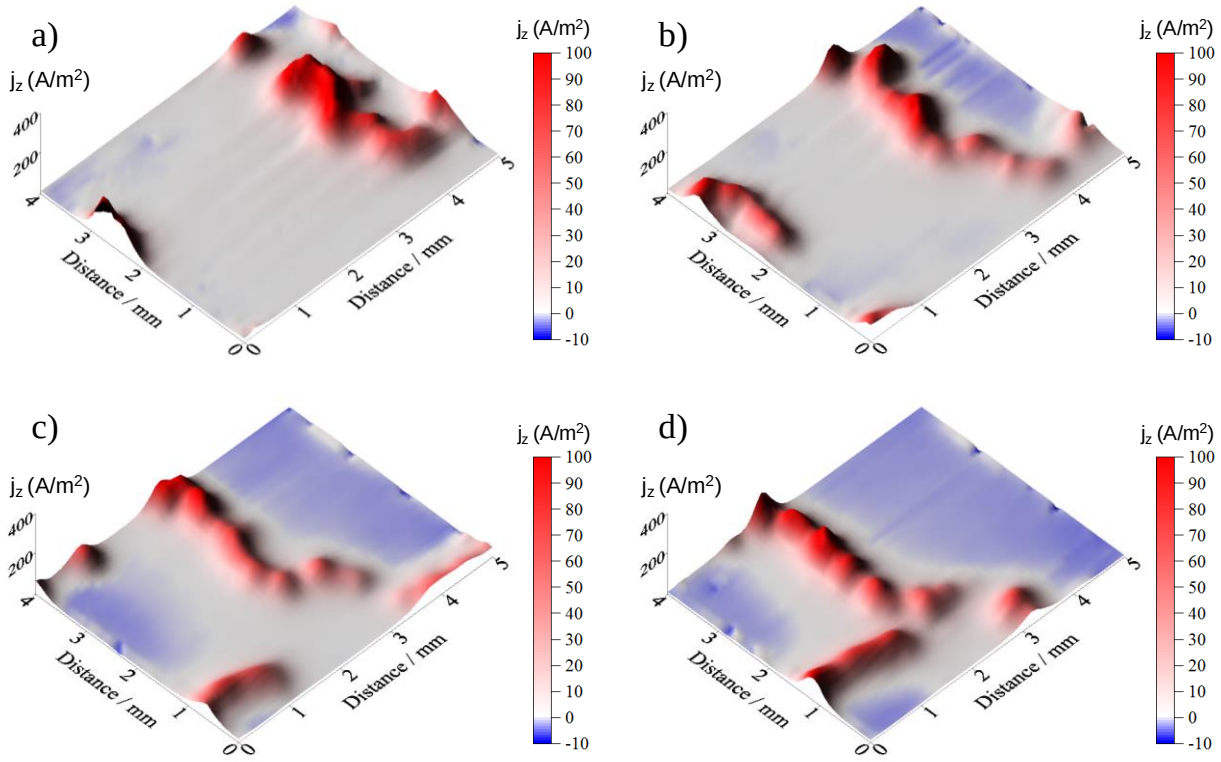

Fig. 2.Surface maps showing normal current density (j_z) distributions above a UHP Mg surface immersed in a 2 M NaCl solution, (a) 7, (b) 21, (c) 35 and (d) 56 min after starting galvanostatic polarization at +2 mA cm^{-2}. A net charge of 6 C cm^{-2} was passed.

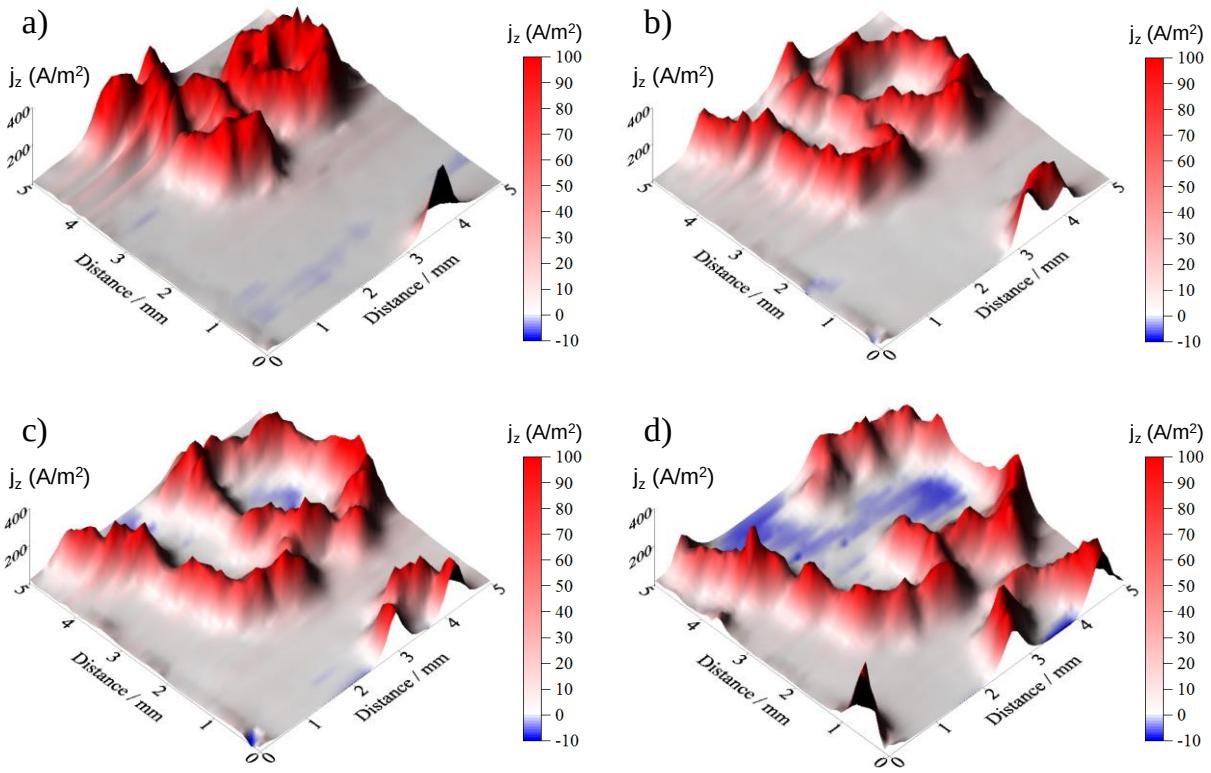

Fig. 3. Surface maps showing normal current density (j_z) distributions above a UHP Mg surface immersed in a 2 M NaCl solution, (a) 6, (b) 12, (c) 18 and (d) 24 min after starting galvanostatic polarization at +4 mA cm^{-2}. A net charge of 6 C cm^{-2} was passed.

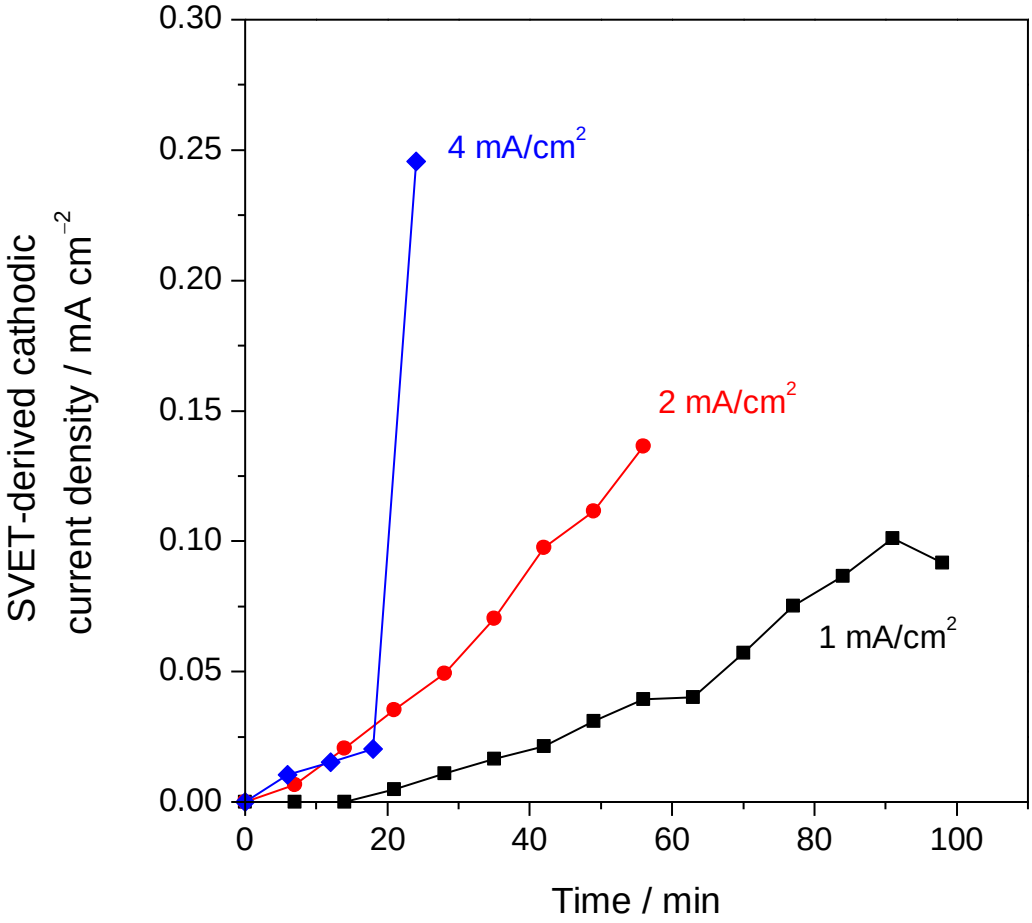

Fig. 4. SVET-derived integrated cathodic current density emerging from a UHP Mg surface in 2 M NaCl solution under anodic galvanostatic polarization at different anodic current densities plotted as a function of time. Current density is presented as absolute value.

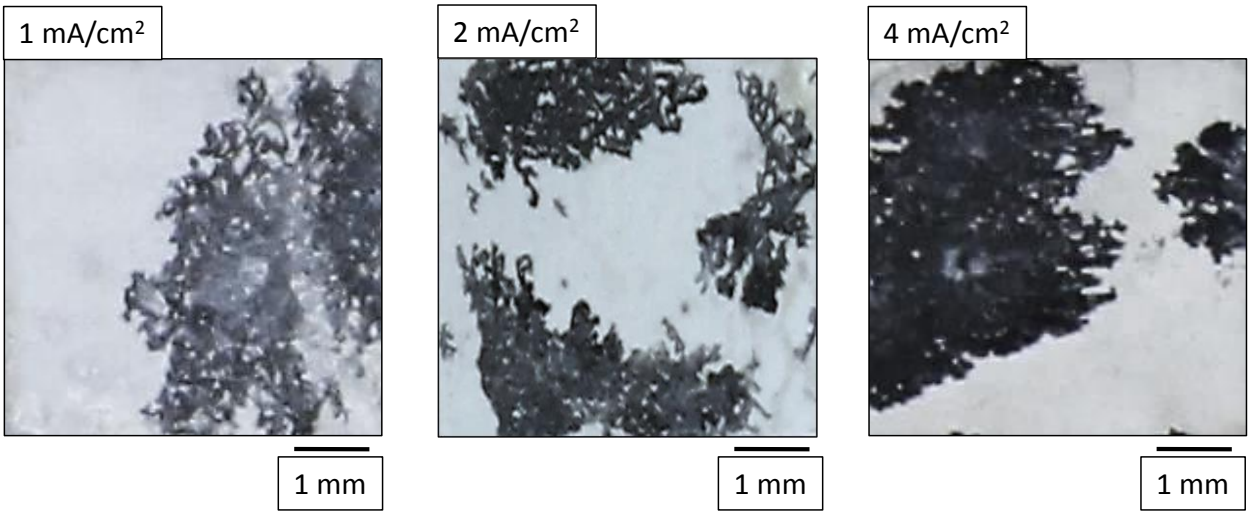

Fig. 5. Surface appearance of the UHP Mg electrode after the SVET measurements where different anodic current densities were applied in 2 M NaCl solution. A net charge of 6 C cm^{-2} was passed.

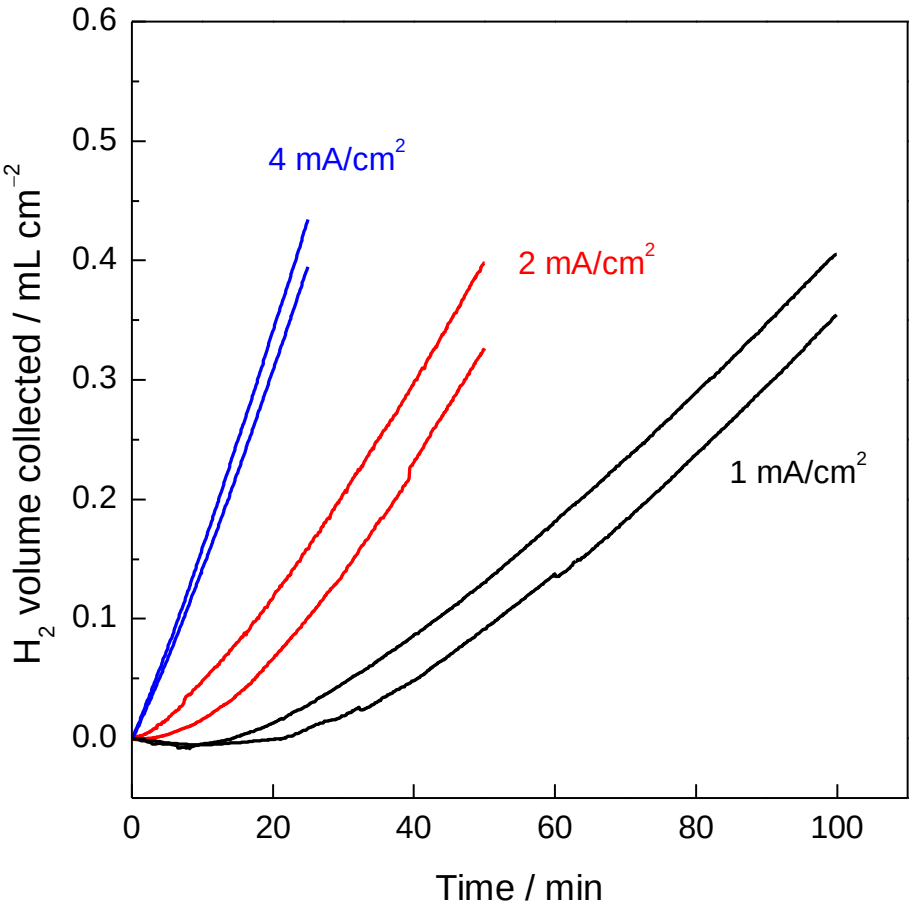

Fig. 6. Volume of hydrogen determined from gravimetric measurements as a function of time for the UHP Mg electrode in 2 M NaCl solution using the gravimetric method for H_2 collection under the application of different anodic current densities. Data from duplicated experiments are presented. A net charge of 6 C cm^{-2} was passed.

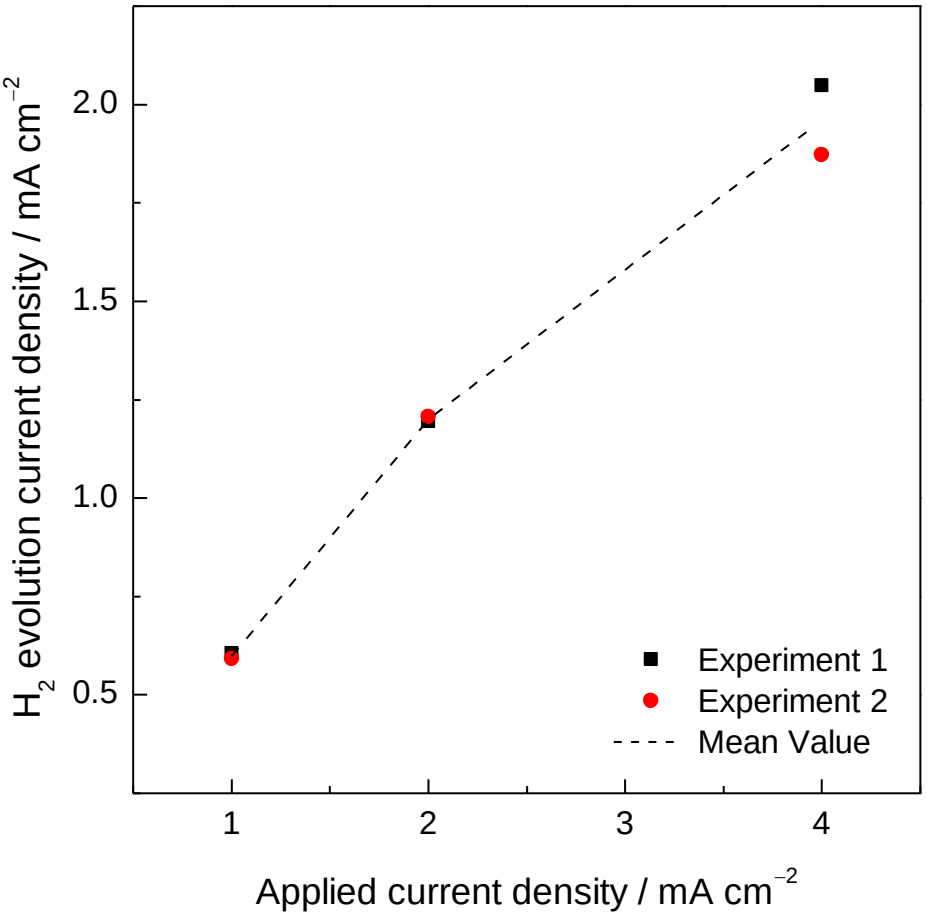

Fig. 7. Current density associated with HE for the UHP Mg electrode in 2 M NaCl solution as a function of the applied anodic current density. Hydrogen evolution current density values were calculated from the steady-state HE rates during galvanostatic polarization measurements using the gravimetric method (Fig.6). Current density is presented as absolute value.

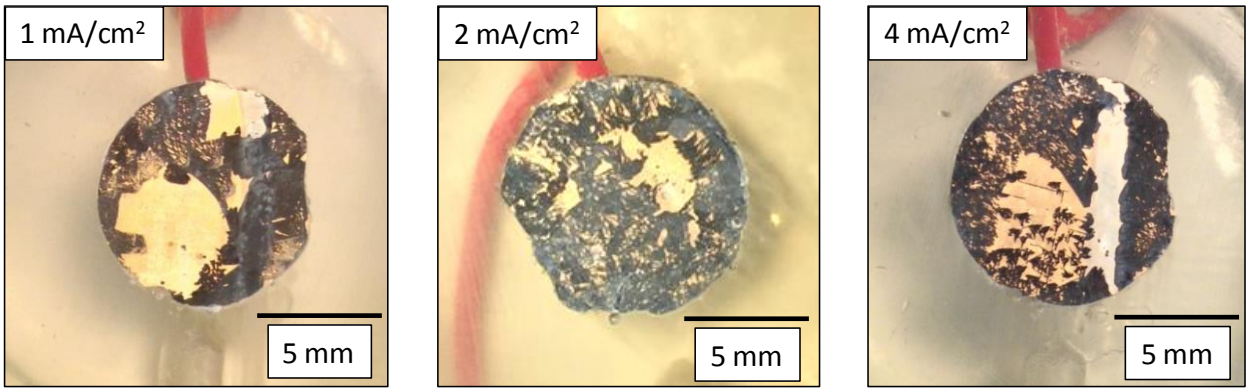

Fig. 8. Surface appearance of the UHP Mg electrode after the application of different anodic current densities in 2 M NaCl solution.

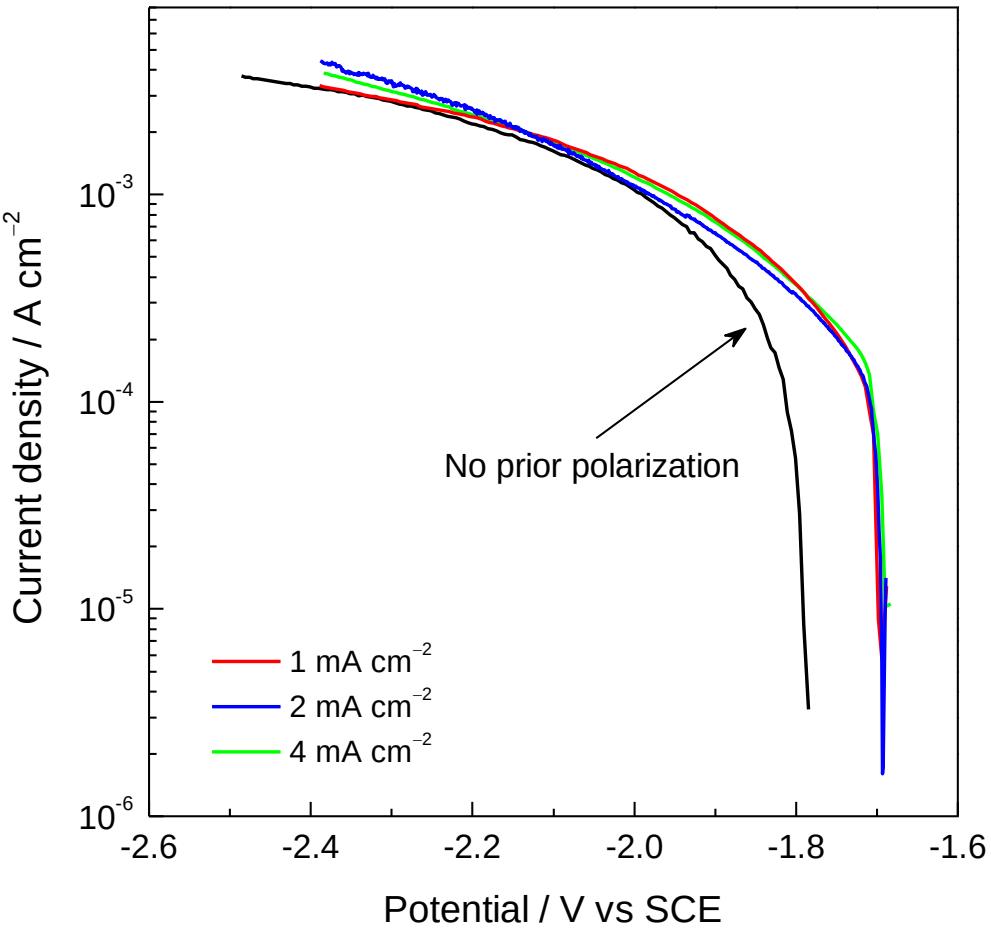

Fig. 9. Cathodic potentiodynamic polarization curves for the UHP Mg electrode in 2 M NaCl solution after galvanostatic polarization at different anodic current densities. Experiments were performed scanning 700 mV downwards from the OCP at a potential scan rate of 1 mV/s. Cathodic potentiodynamic polarization measurements were carried out immediately after prior anodic polarization was finished. Current density is presented as absolute value.

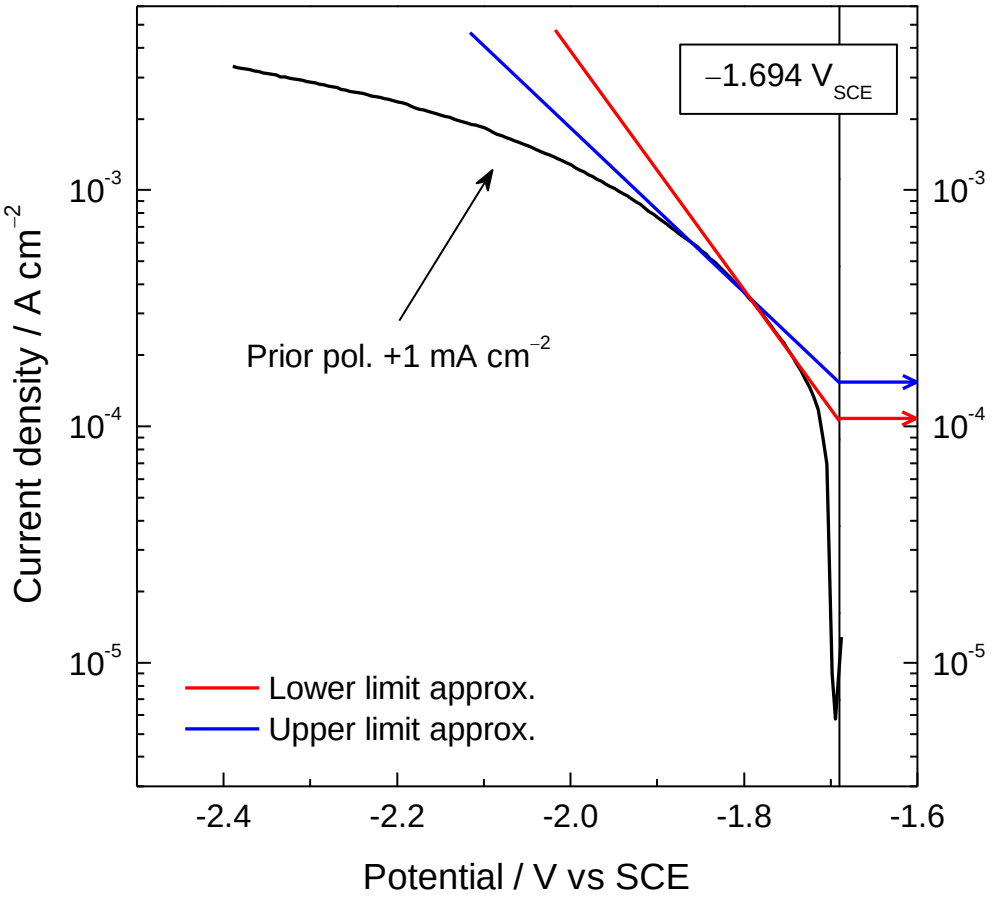

Fig. 10. Determination of hydrogen evolution current density associated with the corrosion product and accumulation of noble impurities for the UHP Mg electrode in 2 M NaCl under the application of different anodic current densities. Determination consisted in extrapolating the cathodic Tafel line to the steady-state reached during anodic polarization. Given the limitations in the determination of a linear region to extrapolate the Tafel line due to ohmic drop effects, two different approximations were considered (i.e. upper and lower limit).

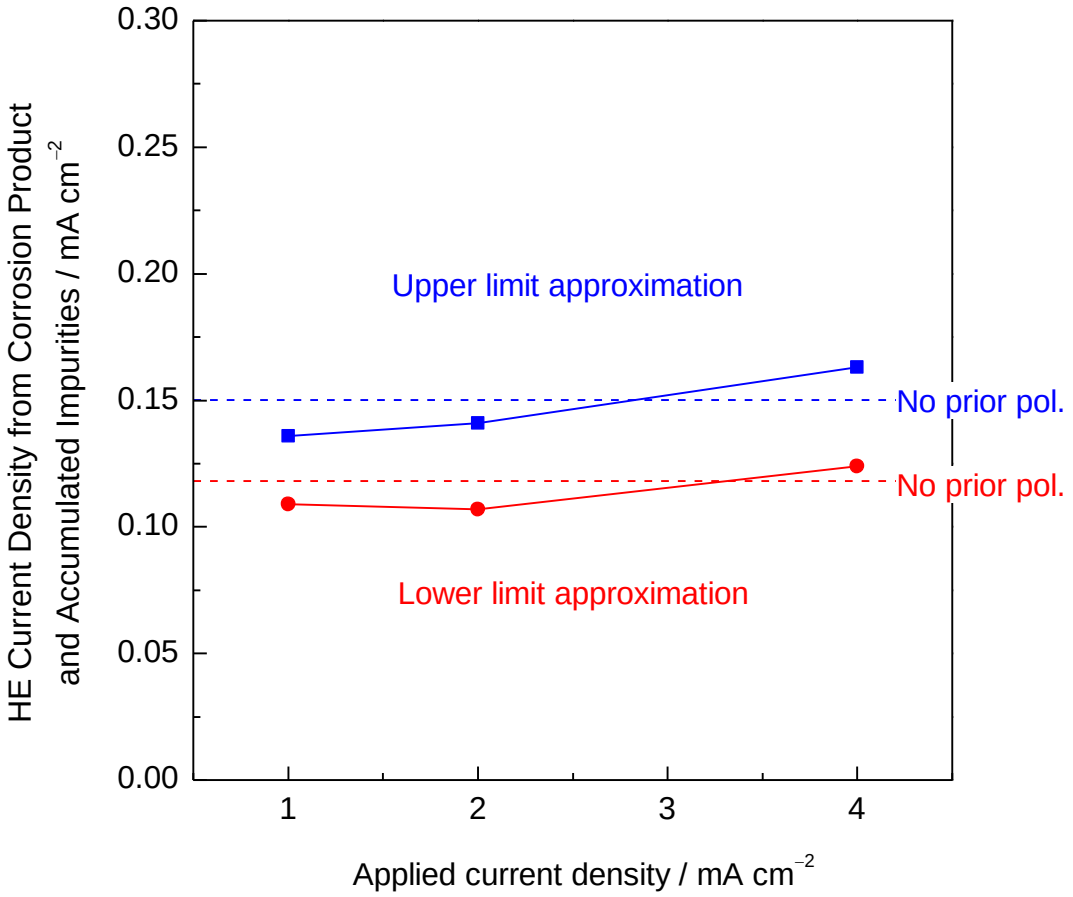

Fig. 11. Hydrogen evolution current density associated with the corrosion product and accumulation of noble impurities for the UHP Mg electrode in 2 M NaCl under the application of different anodic current densities. Current density is presented as absolute value.

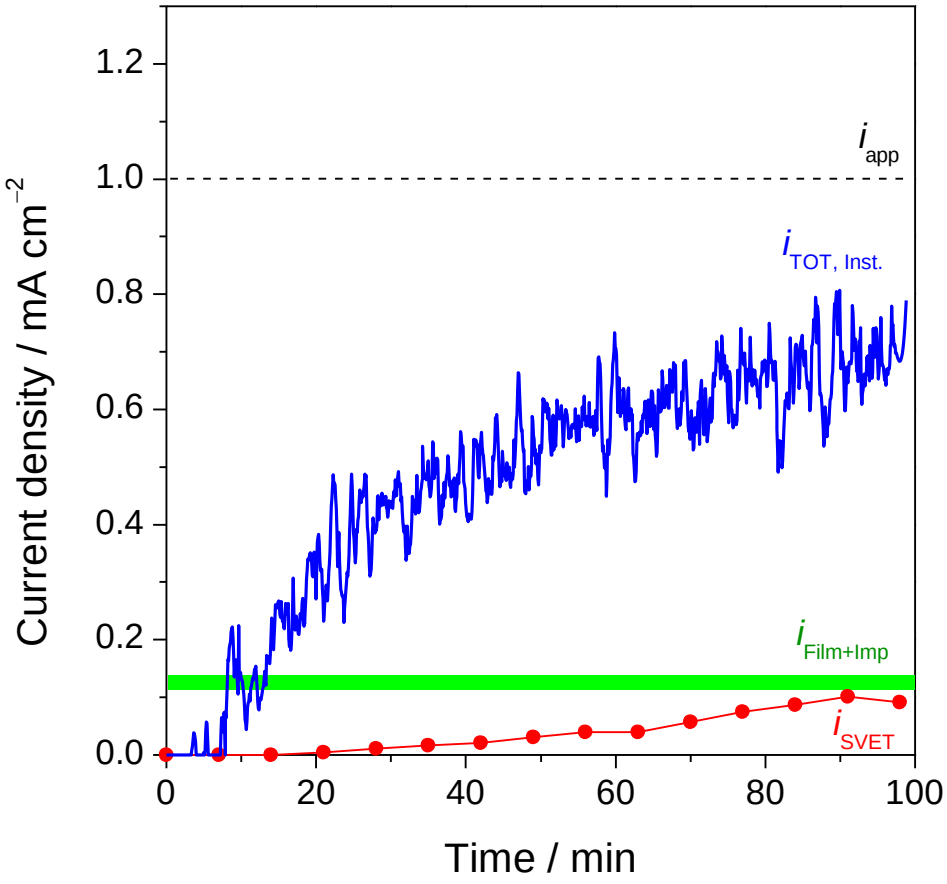

Fig. 12. SVET-derived integrated cathodic current density (i_{SVET}) emerging from a UHP Mg surface under galvanostatic polarization at +1 mA cm^{-2} in 2 M NaCl solution plotted as a function of time (red circles). Dashed line is the net anodic current density applied (i_{app}). Solid blue line is the instantaneous current density associated with HE ($i_{TOT,Inst.}$) obtained using the gravimetric method. Solid green is the hydrogen evolution current density associated with the corrosion product and accumulation of noble impurities ($i_{Film+Imp.}$) from Fig. 11. Current density is presented as absolute value.

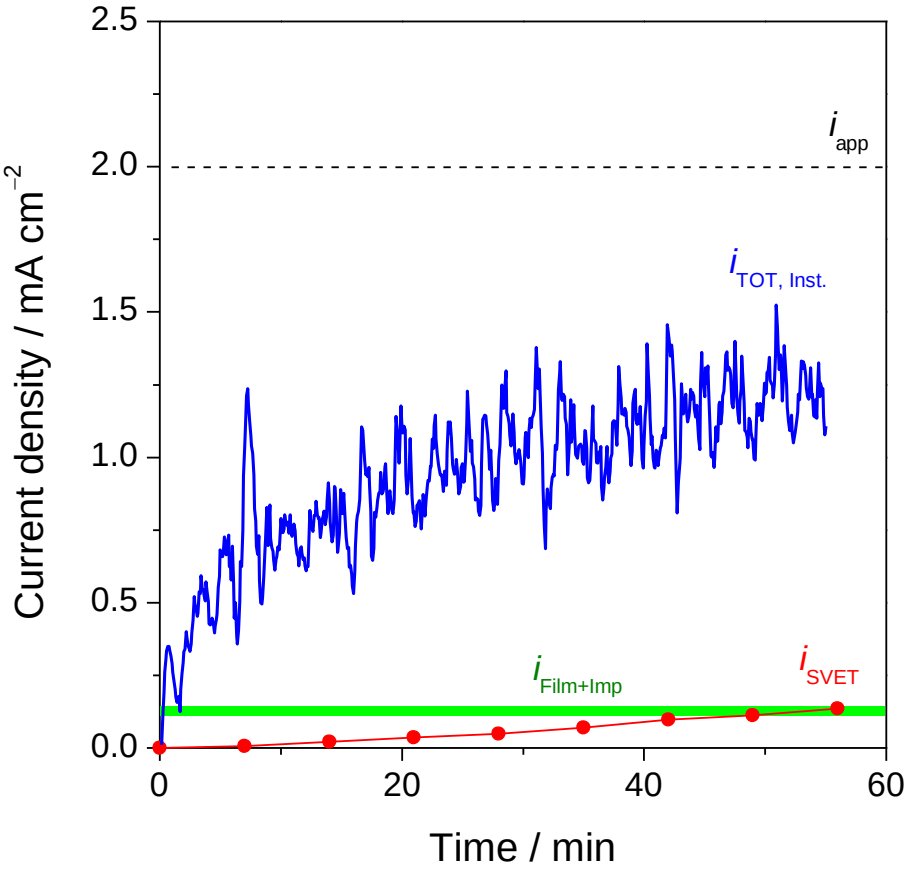

Fig. 13. SVET-derived integrated cathodic current density (i_{SVET}) emerging from a UHP Mg surface under galvanostatic polarization at +2 mA cm^{-2} in 2 M NaCl solution plotted as a function of time (red circles). Dashed line is the net anodic current density applied (i_{app}). Solid blue line is the instantaneous current density associated with HE ($i_{TOT,Inst.}$) obtained using the gravimetric method. Solid green is the hydrogen evolution current density associated with the corrosion product and accumulation of noble impurities ($i_{Film+Imp.}$) from Fig. 11. Current density is presented as absolute value.

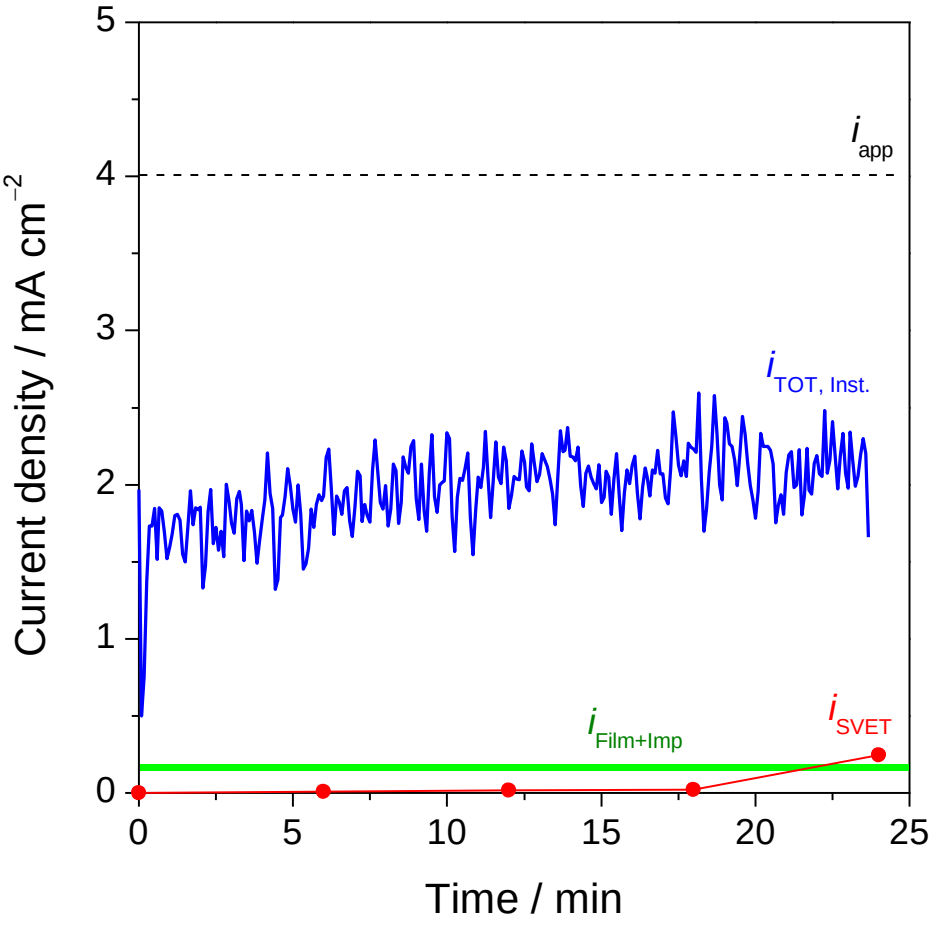

Fig. 14. SVET-derived integrated cathodic current density (i_{SVET}) emerging from a UHP Mg surface under galvanostatic polarization at +4 mA cm^{-2} in 2 M NaCl solution plotted as a function of time (red circles). Dashed line is the net anodic current density applied (i_{app}). Solid blue line is the instantaneous current density associated with HE ($i_{TOT,Inst.}$) obtained using the gravimetric method. Solid green is the hydrogen evolution current density associated with the corrosion product and accumulation of noble impurities ($i_{Film+Imp.}$) from Fig. 11. Current density is presented as absolute value.

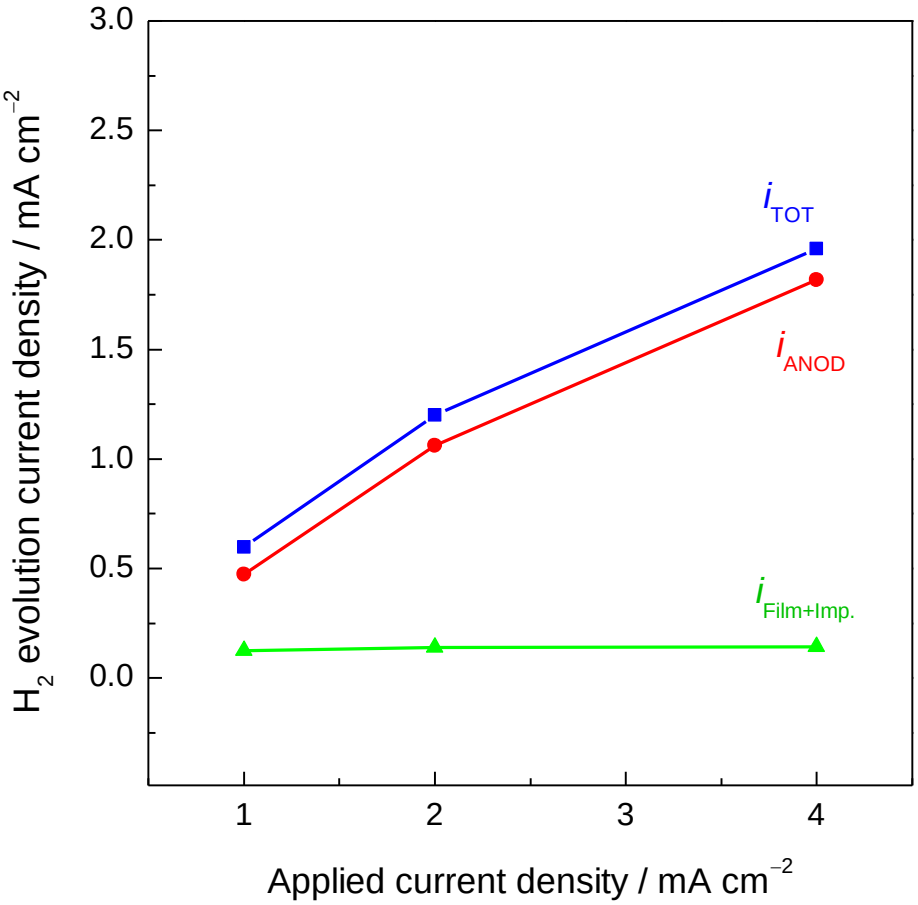

Fig. 15. Hydrogen evolution current density for the UHP Mg in 2 M NaCl solution plotted as a function of the applied anodic current density. Blue squares are the total HE current density calculated from the steady state HE rate using the gravimetric method (i_{TOT}) from Fig. 7. Red circles are the HE current density associated with the regions dominated by the anodic Mg dissolution reaction ($i_{Anod.}$). Green triangles are the mean value of the upper and lower limit HE current density values associated with the corrosion product and accumulation of noble impurities ($i_{Film+Imp.}$) from Fig. 11. Current density is presented as absolute value.

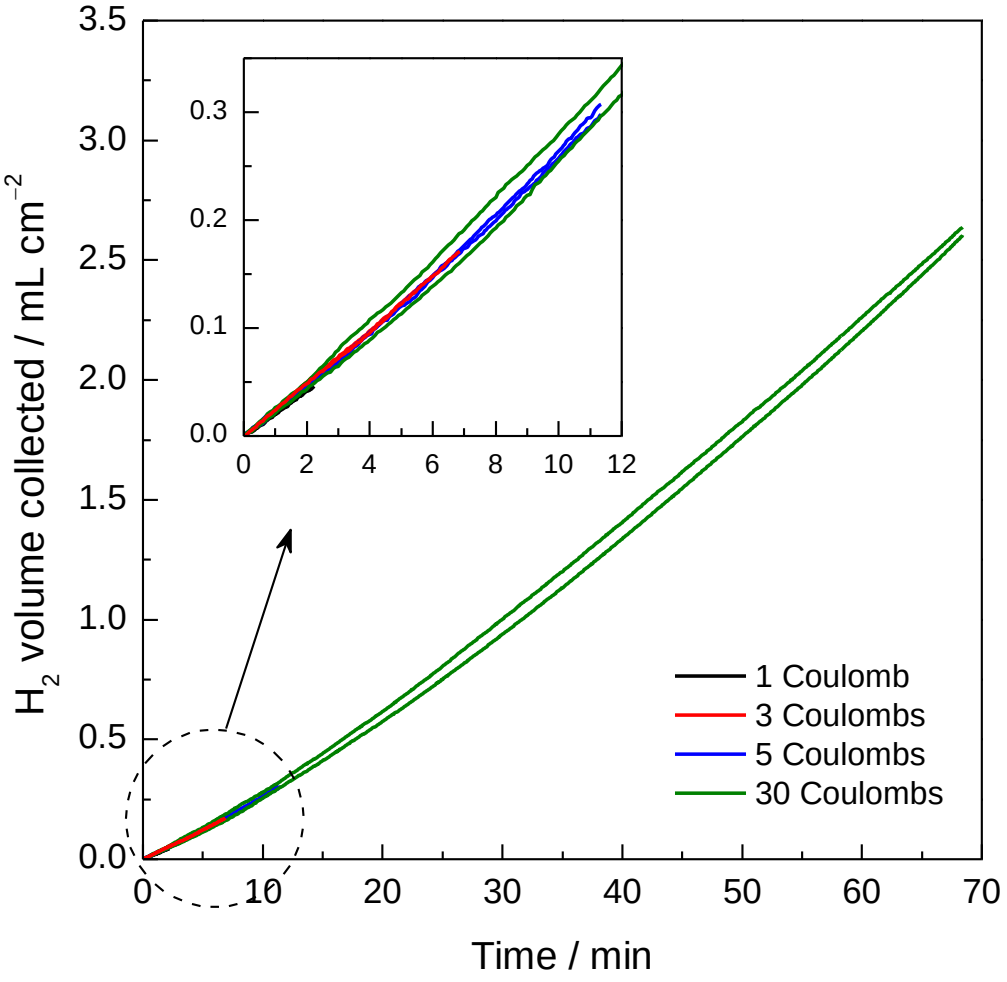

Fig. 16. Volume of hydrogen collected as a function of time for the UHP Mg electrode in 0.1 M NaCl solution using the gravimetric setup for HE collection. Different charges in the range of 1 to 30 Coulombs were passed at constant anodic current density of 10 mA cm^{-2}. Data from duplicated experiments are presented.

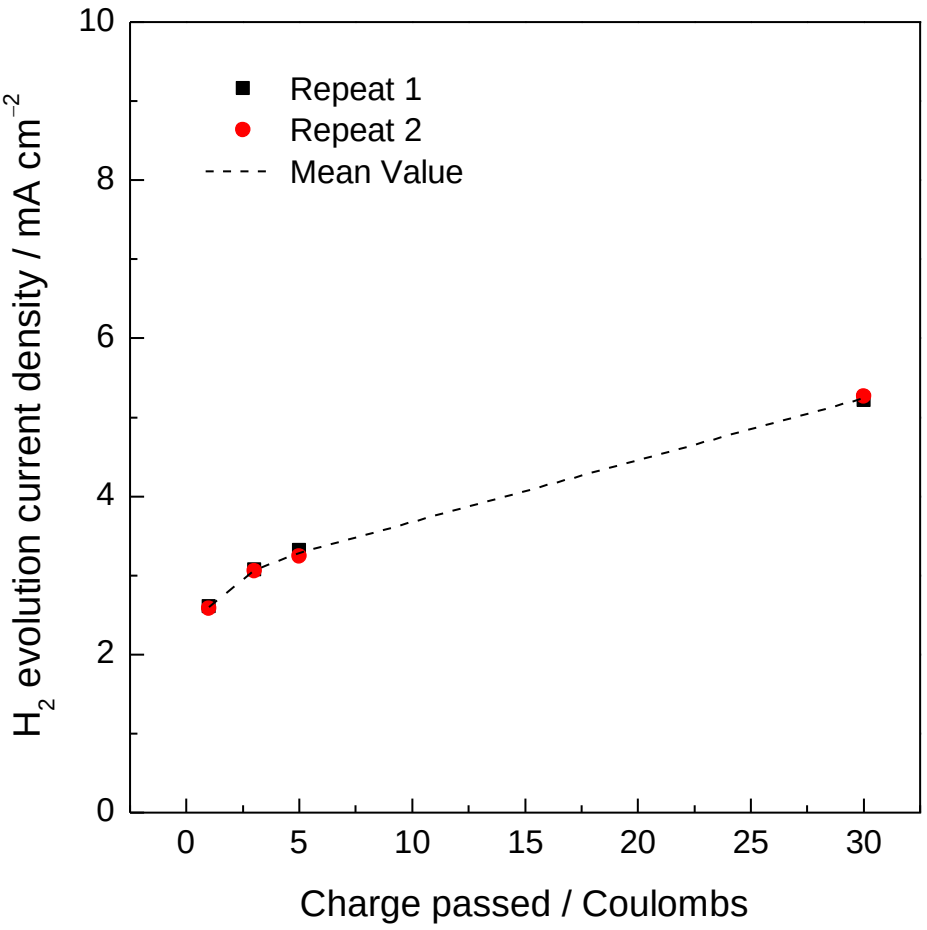

Fig. 17. Current density associated with HE for the UHP Mg electrode in 0.1 M NaCl solution as a function of anodic charge passed. Hydrogen evolution current density values were calculated from the steady-state HE rates during galvanostatic polarization measurements using the gravimetric method (Fig.16). Current density is presented as absolute value.

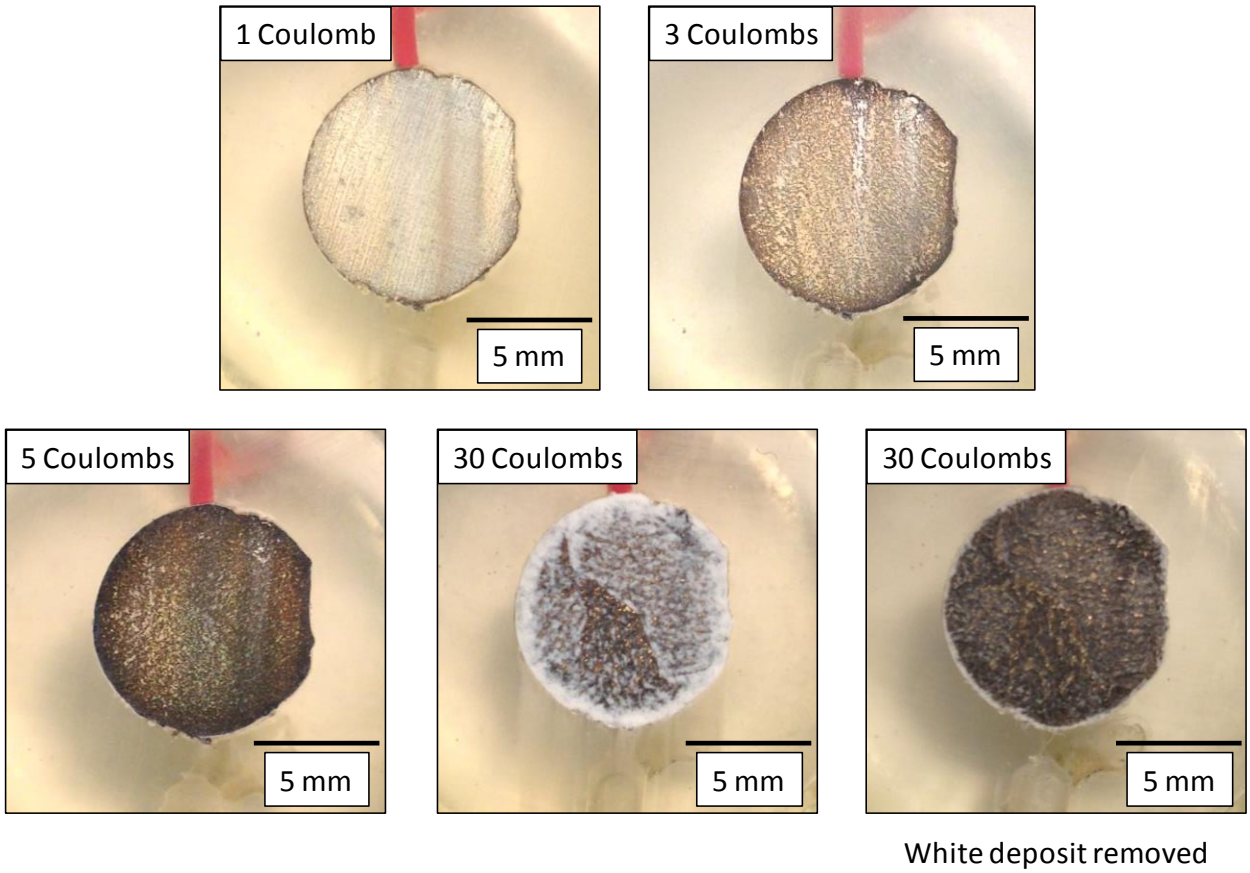

Fig. 18. Surface appearance of the UHP Mg electrode after passing different charges at a constant anodic current density of 10 mA cm^{-2} in 0.1 M NaCl solution.

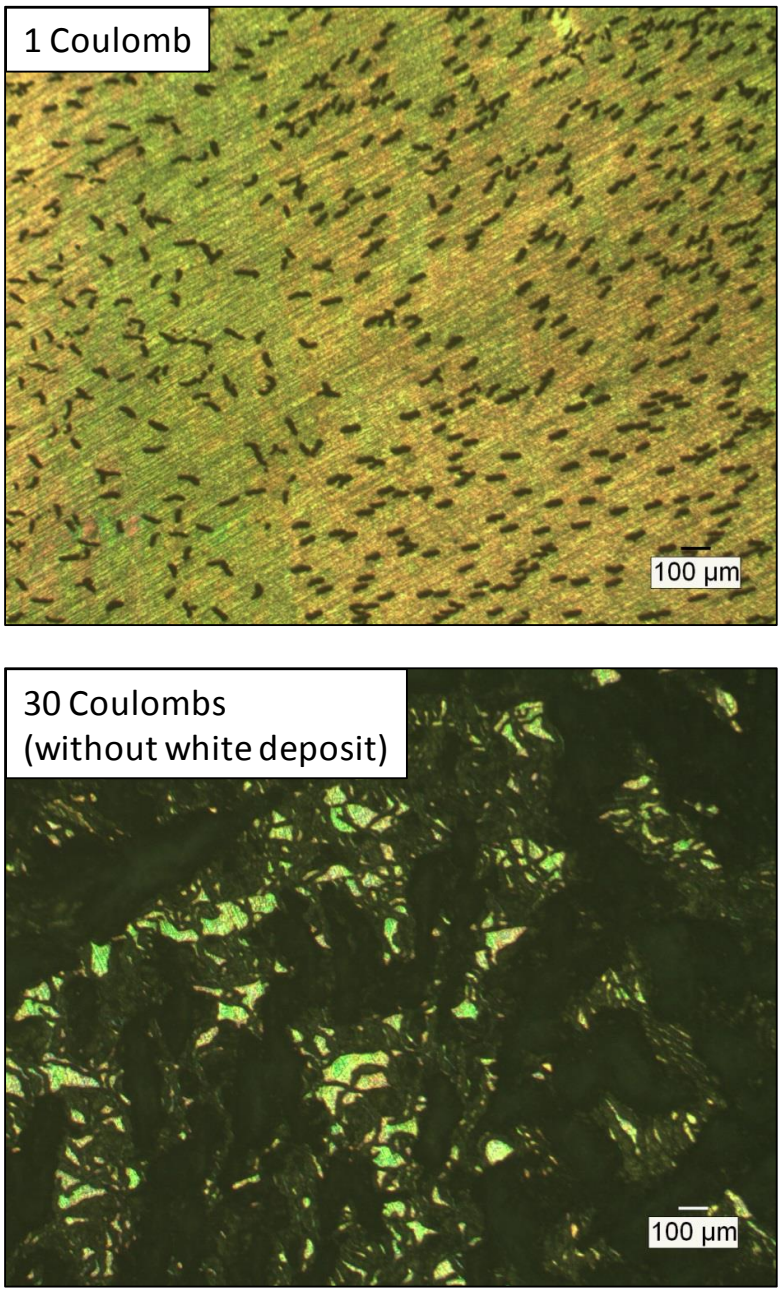

Fig. 19. Optical micrograph of the surface of the UHP Mg electrode after passing 1 and 30 Coulombs at a constant anodic current density of 10 mA cm^{-2} in 0.1 M NaCl solution.

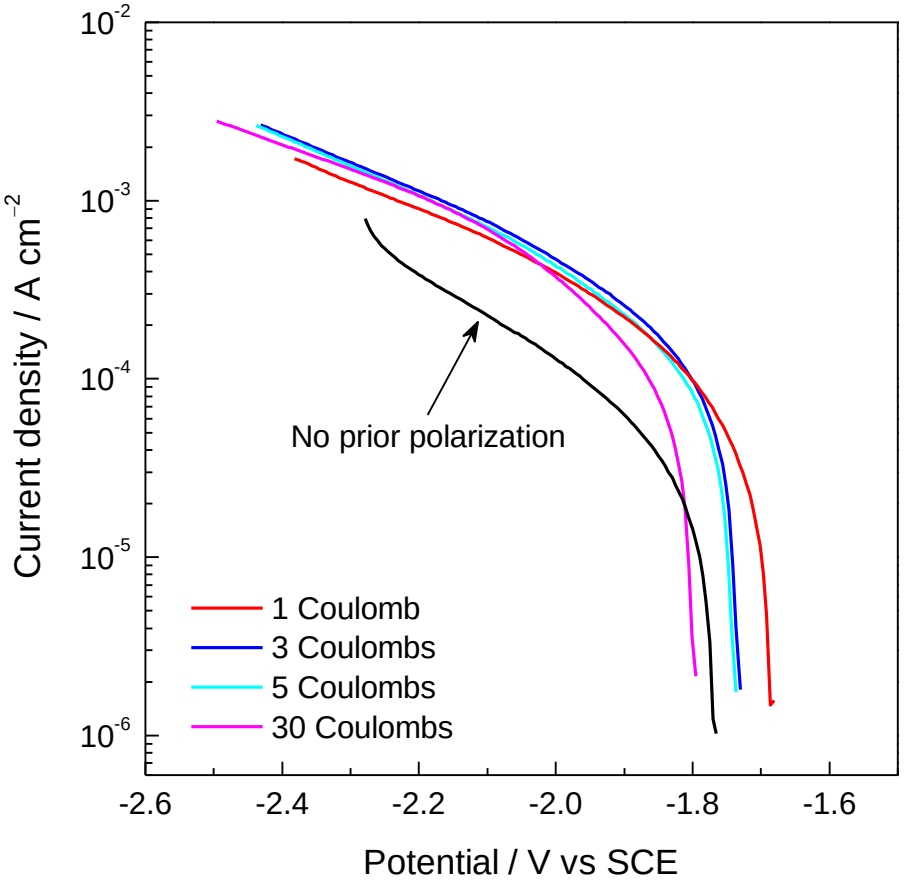

Fig. 20. Cathodic potentiodynamic polarization curves for the UHP Mg electrode in 0.1 M NaCl solution after galvanostatic polarization passing different charges at constant anodic current density of 10 mA cm^{-2}. Experiments were performed starting from the OCP at a potential scan rate of 1 mV/s. Current density is presented as absolute value.